Tangeretin Mitigates Trimethylamine Oxide Induced Arterial Inflammation by Disrupting Choline-Trimethylamine Conversion through Specific Manipulation of Intestinal Microflora

Yu Cao , Changlong Leng , Kuan Lin , Youwei Li , Meiling Zhou , Mei Zhou , Xi-ji Shu , Wei Liu *

Posted Date: 12 January 2024

doi: 10.20944/preprints202401.0960.v1

Keywords: TMA; tangeretin; CutC; vascular inflammation

Article

Tangeretin Mitigates Trimethylamine Oxide Induced Arterial Inflammation by Disrupting Choline-Trimethylamine Conversion through Specific Manipulation of Intestinal Microflora

Yu Cao [1], Changlong Leng [1,2], Kuan Lin [1,2], Youwei Li [1], Meiling Zhou [1,2], Mei Zhou [1,2], Xiji Shu [1]* and Wei Liu [1,2,]*

[1] Wuhan Institute of Biomedical Sciences, School of Medicine, Jianghan University, Wuhan 430056, Hubei, China.

[2] Institute of Cerebrovascular Disease, School of Medicine, Jianghan University, Wuhan 430056, Hubei, China.

* Correspondence: author: W Liu, Tel: (+86) 027-84225417, Email address: liuwei@jhun.edu.cn; X Shu, Tel: (+86) 027-84226723, Email address: xijishu@jhun.edu.cn.

Highlights:

1. Tangeretin demonstrates a preventative effect against choline-induced cardiovascular inflammation.
2. Tangeretin inhibits CutC activity, consequently hindering the conversion of choline to trimethylamine (TMA).
3. The inhibitory efficacy of tangeretin is related to its interference in gut microbiota-mediated conversion of choline to TMA.

Abstract: Previous studies have revealed the microbial metabolism of dietary choline in the gut, leading to its conversion into trimethylamine (TMA), a precursor of the cardiovascular inflammatory marker trimethylamine N-oxide (TMAO). Polymethoxyflavones (PMFs), exemplified by tangeretin, demonstrate efficacy in mitigating TMAO-induced cardiovascular inflammation. However, the specific mechanism by which these compounds exert their effects, particularly in modulating the gut microbiota, remains uncertain. This investigation focused on tangeretin, a representative PMFs, exploring its influence on the gut microbiota and the choline-TMA conversion process. Experimental results showed that tangeretin treatment attenuated the population of CutC-active bacteria, specifically *Clostridiaceae* and *Lactobacillus*, induced by choline chloride in rat models. This inhibition resulted in reduced efficiency in choline conversion to TMA, thereby ameliorating cardiovascular inflammation resulting from prolonged choline consumption. In conclusion, tangeretin's preventive action against cardiovascular inflammation is intricately linked to its targeted modulation of TMA-producing bacterial activity.

Graphic Abstract

Preprints (www.preprints.org) | NOT PEER-REVIEWED | Posted: 12 January 2024 doi:10.20944/preprints202401.0960.v1

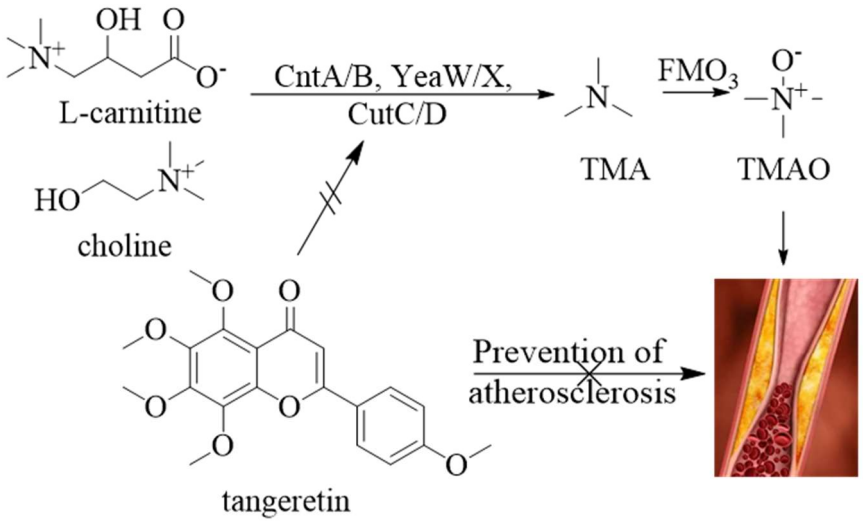

Keywords: TMA; tangeretin; CutC; vascular inflammation

1. Introduction

In recent years, the prevalence of metabolic syndromes, including cardiovascular disorders, obesity, and diabetes, has surged, becoming a pressing societal concern [1]. Research indicates that, beyond genetic factors, this surge is associated with the increasing westernization of dietary patterns. Specifically, there has been a shift towards elevated consumption of meat and fats, encompassing red meat, eggs, soybeans, and other trimethylamine (TMA) substitute-rich foods [2]. While traditional nutritional science implicates red meat, egg yolk, liver, and choline-rich soybeans in cardiovascular risk, recent publications in esteemed journals such as Nature [3], Nature Medicine [4], and the New England Journal of Medicine [5] propose that dietary choline may significantly elevate the risk of cardiovascular disease. This connection is primarily attributed to the transformation of choline and its derivatives into TMA by gut bacteria during digestion and absorption, subsequently oxidizing into trimethylamine oxide (TMAO). Multiple studies confirm the detrimental impact of TMAO on cardiovascular cells, promoting atherosclerosis, a crucial factor in atherosclerosis development [3, 6, 7].

Individuals with atherosclerosis exhibit significantly higher TMAO levels in their blood samples compared to those without the condition [4]. Notably, two dominant CutC species, *Lachnoclostridium* (p = 2.9e-05) and *Clostridium* (p = 5.8e-04), were found to be elevated in atherosclerotic patients compared to their healthy counterparts. *L. saccharolyticum*, when exposed to choline as a substrate, converted it effectively to TMA, with a conversion rate of up to 98.7% [8]. This underscores the role of gut microbiota disruption in TMAO formation and subsequent induction of atherosclerosis. Microbial TMA lyase activity, responsible for TMAO production, further supports the link between gut microbiota and atherosclerosis development [7, 9]. Jonsson et al.'s study [9] indicated that the impact of gut microbiota on atherosclerosis is diet-dependent, and single choline supplementation does not influence plaque size and aortic lesions. The gut microbiota utilizes three TMA lyase complexes, CntA/B, YeaW/X, and CutC/D, to convert carnitine, betaine, and choline into TMA, with CntA, YeaW, and CutC being lyases, and CntB, YeaX, and CutD acting as their activators. The relative abundance of CutC significantly increased in atherosclerosis patients (p = 0.033), suggesting its potential association with atherosclerosis formation [8].

The citrus peel's unique polymethoxyflavones (PMFs), such as nobiletin and tangeretin [10], exhibit the ability to inhibit TMAO generation *in vivo*. Yang et al.'s study [2] revealed that administration of nobiletin mitigated choline-induced oxidative damage in the proximal aorta of experimental rats. It suppresses MAPK/ERK activity, reduces the expression of NF-κB p65 and phosphorylated NF-κB p65, thereby diminishing inflammation. Nobiletin also demonstrated the

 doi:10.20944/preprints202401.0960.v1

ability to reduce TMAO-induced apoptosis of HUVEC cells and inhibit TMAO-induced proliferation of HUVEC cells. However, the study did not elucidate the regulatory mechanism of nobiletin on TMAO generation. Zhang et al. [11, 12] discovered that nobiletin actively modulates gut microbiota composition, particularly affecting *Allobaculum* and *Roseburia*. These findings suggest that PMFs, as major active components of citrus peel, possess the potential to shape gut microbiota structure and hinder the biological activity of TMA production.

Therefore, our study aims to investigate the targeted modulation of gut microbiota composition by tangeretin, another prominent PMF similar to nobiletin, with a focus on inhibiting TMA generation and preventing the biological activity of arterial tissue inflammation.

2. Materials and Methods

2.1. Materials and Reagents

Tangeretin, with a minimum purity of 98%, was procured from Kang Biotech (Changsha, Hunan, China). High-quality reagents, including TMA, 99% pure choline chloride, TMAO, and hematoxylin & eosin (HE), were sourced from Sigma-Aldrich (St. Louis, MO, USA). 3,3-Dimethylbutanol (DMB), 4% paraformaldehyde, and Oil Red O were obtained from Beyotime Biotechnology (Shanghai, China). Cholesterol package, superoxide dismutase activity colorimetric assay kit, and triglyceride package were acquired from Nanjing Jiancheng Bioengineering Institute Co., Ltd. (Nanjing, Jiangsu Province, China).

2.2. Experimental Animal Model

Fifty Sprague-Dawley (SD) male rats (ages 4-6 weeks) were obtained from the Hubei Research Center of Laboratory Animals (Wuhan, Hubei, China). Rats were provided unrestricted access to nourishment and water. After one week of acclimatization, the rats were randomly assigned to six groups, each containing 7-8 animals: normal group (NOR), TMA positive group (TMA), choline model group (CHO), low tangeretin exposure group (LTN), medium tangeretin exposure group (MTN), and high tangeretin exposure group (HTN). All groups, except for NOR and TMA, received drinking water enriched with 3% choline chloride. The exposure groups were subjected to intragastric administration of 50 (LTN), 100 (MTN), or 200 (HTN) mg/kg body weight (BW) of tangeretin suspended in a 1% sodium carboxymethyl cellulose aqueous solution (1 mL/dose, once daily). Experimental procedures strictly followed the ethical guidelines outlined in the European Parliament Directive on the Conservation of Animals Used for Scientific Studies (Directive 2010/63/EU) and the NIH Guide for the Care and Use of Laboratory Animals, under authorization No JHDXLL0-46 from the Experimental Animal Ethics Committee of Jianghan University.

After a 6-week period, nocturnal fasting rodents were sedated with 4% isoflurane, and blood samples were withdrawn from the left ventricle for quantitative assessment of total cholesterol (TC), triglycerides (TG), high-density lipoprotein cholesterol (HDL-C), low-density lipoprotein cholesterol (LDL-C), aspartate transaminase (AST), and alanine transaminase (ALT) using commercial kits (Jiancheng Biotechnology Co., Ltd.). Simultaneously, fecal matter was collected and stored at -80°C for subsequent analysis, while the ileum and aortic tissues were promptly excised, submerged in cold physiological saline, and either stored at -80°C or embedded in 4% paraformaldehyde for histopathological examination.

2.3. Histomorphological Staining

Specimens of the terminal ileum (proximal ileocecal valve) and proximal aortic arch were fixed in a 4% paraformaldehyde solution. Standard paraffin embedding, dewaxing, and sectioning protocols were followed by HE staining. Pathological examination was conducted using a BH2 optical microscope (200× magnification, Olympus, Hino, Tokyo, Japan).

2.4. Immunohistochemical Detection

 doi:10.20944/preprints202401.0960.v1

Thin sections of paraffin-embedded tissue were transferred onto gelatine-coated microscope slides. After deparaffinization, rehydration, and inactivation, sections were incubated overnight with primary antibodies (Zonula Occludens-1, ZO-1, Catalogue # 21773-1-AP or Occludin, Catalogue # 13409-1-AP from Proteintech, Wuhan, Hubei, China). Following three washes with phosphate buffer, slices were exposed to HRP secondary antibody (Catalogue # ab205718, Abcam, Cambridge, MA, USA). Specimens were stained with the chromogenic reagent 3,3′-diaminobenzidine (DAB) (Sigma-Aldrich) and counterstained with hematoxylin. The proportion of positively stained cells at each intensity level was measured using the H-score method according to the following formula: H score = 1 × (% mild staining) + 2 × (% moderate staining) + 3 × (% strong staining).

2.5. RNA Isolation and Quantitative RT-qPCR

Aortic tissue was homogenized using liquid nitrogen, and total RNA was isolated with TransZol-Up reagent (TransGen Biotech Co., Ltd., Beijing, China). RNA quality, purity, and concentration were assessed using a Nanodrop 2000C ultra-micro spectrophotometer (BIO-RAD T100, Hercules, CA, USA). Reversely transcribed cDNA was synthesized from approximately 1 μg of total RNA using a HiScript™ Q RT SuperMix kit (Vazyme, Shanghai, China). Real-time quantitative polymerase chain reaction (RT-qPCR) was performed with a CFX96 real-time PCR system (ABI, Foster City, CA, USA) for Toll-like receptor 4 (TLR4), Myeloid differentiation primary response 88 (MyD88), and Nuclear factor kappa-light-chain-enhancer of activated B cells (NF-κB) target genes. GAPDH served as a control. The primer sequences are delineated in **Table 1**, and the relative expressions of target genes were calculated using the $2^{-\Delta\Delta Ct}$ method.

Table 1. Primers used in the RT-qPCR.

Gene name	Forward primer (5'-3')	Reverse primer (5'-3')
TLR4	GAGGACTGGGTGAGAAACGA	GCAATGGCTACACCAGGAAT
MyD88	TGTGTGTTTCCTTTGGGACA	TGCCACTACCTCATGCAAAG
NF-κB	GATGCAGTTAATGCCCCACT	TGCTGCTGGTGATTCTCTTG
GAPDH	ATGACTCTACCCACGGCAAG	GATCTCGCTCCTGGAAGATG

2.6. Cytokine Analysis

Serum cytokine profiling, including TNF-α, IL-1β, IL-6, IL-10, and IL-17, was conducted on serum samples using ELISA (Bio-Swamp, Wuhan, Hubei, China) following the provided protocol. Optical density (OD) values at a wavelength of 450 nm were measured using a microtiter plate reader (LabSystems, Helsinki, Finland).

2.7. Intestinal Microbiota Sequencing Procedure

The exclusive DNeasy PowerSoil Kit (Qiagen, Dusseldorf, Germany) facilitated comprehensive DNA extraction from ileal content for microbiome characterization. This extraction involved crucial steps: DNA quantification using the sophisticated NanoDrop ND-1000 spectrophotometer (Plant & Life Science, Waltham, MA, USA), followed by electrophoresis examination via agarose gel imaging to determine purity. The bacterial taxa were amplified using fragments of the V3-V4 variable restriction fragment of the 16S RNA gene with primers 338F (5'- barcode+

 doi:10.20944/preprints202401.0960.v1

ACTCCTACGGGAGGCAGCA -3') and 806R (5'- GGACTACHVGGGTWTCTAAT -3'). The purification of PCR products employed beads from Agencourt AMPure (Beckman Coulter, Brea, CA, USA). Post-extraction, quantification was assessed using a PicoGreen dsDNA Assay Kit (Invitrogen, Carlsbad, CA, USA). Depending on product yield, multiplexed 2×300 bp sequencing occurs on an Illumina MiSeq instrument using the latest MiSeq Reagent Kit v3, provided by Wuhan Servicebio Technology Co., Ltd. (Wuhan, Hubai, China).

For quality control, the Quantitative Insights into Microbial Ecology pipeline (version 1.8.0) managed raw FastQ files [13]. Clustering sequence information at 97% sequence identity via UCLUST formed the basis for Operational Taxonomic Units (OTUs) [14]. These OTUs, after being aligned to the respective barcode sequences, resulted in relative abundance ASVs (Feature) data. Subsequent steps catalyzed both α diversity analysis (Chao1 index & Shannon diversity index) and β diversity analysis (PCAs) [15]. The visual representation of these analyses was achieved through principal coordinate analysis (PCoA) using MEGAN [16] and GraPhlAn [17], proprietary tools from BioGraph AG, for visualizing taxonomic compositions and abundance. Visualization of shared and unique OTUs in sample or group comparisons employed the R software package Venn Diagram [18].

2.8. Bacterial Species and Habitats

To assess the *in vitro* efficiency of TMA-proliferating bacteria, *L. saccharolyticum* WM1 (ATCC 35040) was cultured under microaerophilic conditions in ATCC medium 1118 at 37°C. Analyzing the influence of tangeretin on choline transamination into TMA during *L. saccharolyticum* WM1 cultivation involved inoculating microbial populations with choline chloride in sterile vessels. These populations were incubated under microaerobic conditions (composed of 80% N_2 and 20% CO_2) at 37°C until cells attained an optical density at 600 nm (OD600) close to unity. Subsequently, cultures underwent centrifugation at approximately 15,294 ×*g* for 10 min at 4°C.

2.9. Molecular Docking

The amino acid sequence of CutC protein from *L. saccharolyticum* WM1 was extracted from prior scientific literature [8]. Protein topological modeling was pursued using Robetta (https://robetta.bakerlab.org/submit.php), while structural refinement of the protein was performed using I-TASSER (https://zhanglab.ccmb.med.umich.edu/I-TASSER/) online resources. After modeling, the protein constructs were optimized by using Discovery Studio 2.5 software. The protein models were reassessed using the SAVES v6.0 platform (https://saves.mbi.ucla.edu/). Structural data for tangeretin were extracted from the PubChem database (https://pubchem.ncbi.nlm.nih.gov/) and subsequently structurally refined. Computational docking was carried out with the help of Autodock Vina software, and the results were depicted using PyMOL software. Finally, pictorial renderings were formulated using PyMOL (Schrödinger, LLC. The PyMOL molecular graphics system, version 1.8, 2015.).

2.10. Measurement Quantification of TMA and TMAO

TMA in caecal contents and culture supernatant, and TMAO in plasma, were quantified using HPLC-MS/MS. Specifically, 200 mg of ileum content was precisely measured, stirred for 10 min using a solution of acetonitrile: methanol: water (V:V:V = 40:40:20), with 2.0 μM of D9-TMA incorporated into cecal samples as an internal standard. This mixture was agitated, then equilibrated at -80°C for 2 h, and subsequently centrifugated at 15,294 ×*g* for 15 min at 4°C. The supernatant was extracted and filtered through a 0.22 μm membrane for TMA evaluation [19].

For plasma samples, 20 μL of the sample was treated with 80 μL of acetonitrile for protein precipitation. 2.0 μM of D9-TMAO was incorporated into plasma samples as an internal standard. This formulated mixture was agitated, left static at -80°C for 2 h, and subsequently centrifuged at 15,294 ×*g* for 15 min at 4°C. The supernatant was extracted and filtered through a 0.22 μm membrane for TMAO determination [19].

 doi:10.20944/preprints202401.0960.v1

HPLC-MS/MS analysis was performed on a TSQ Quantum Triple Quadrupole Mass Spectrometer (Thermo Fisher Scientific, Waltham, MA, USA) using a Welch Ultimate XB-C8 column (150×4.6 mm, 5 μm, Welch Materials, Inc, Shanghai, China) for separation. The injector temperature was 350°C, with an injection volume of 2.00 μL. High-purity nitrogen (99.999%) was utilized as the carrier gas at a flow rate of 0.8 mL/min. The mobile phase A was consisted of 0.1 mM ammonium formate (pH=3.5), and the mobile phase B was acetonitrile. The elution conditions were as follows: 0-0.15 min, 5% of phase A and 95% of phase B; 0.15-1.2 min, 15% of phase A and 85% of phase B; 1.2-3.0 min, 20% of phase A and 80% of phase B; 3.0-6.0 min, 30% of phase A and 70% of phase B; 6.0-7.0 min, 45% of phase A and 55% of phase B; 7.0-11.0 min, 45% of phase A and 55% of phase B; 11.0-12.0 min, 5% of phase A and 95% of phase B, and sustained at 5% of phase A and 95% of phase B until completion, with a total run time of 15 min.

2.11. Statistical Analysis

We assessed statistical differences between groups using the Wilcoxon rank sum procedure. For multi-group comparison, the Kruskal-Wallis test, supplemented by Holm-Bonferroni adjustment, was implemented. Distinctions between groups in animal experiments were examined through single-factor variance analysis using Tukey HSD. All statistical analyses were performed using the R 3.6.1 package, and values below 0.05 were considered statistically significant.

3. Results and Discussion

3.1. Tangeretin Effectively Counteracted the Negative Effects of Choline Chloride-Induced Inflammation

Histological analyses (**Figure 1**A) showed that rats treated with choline chloride displayed intimal thickening, shedding of endothelial tissue, and localized elevation of the aortic intima near the heart. In addition, proliferation of elastic fibers in the aorta tunica media was observed, along with vacuolar degeneration in the intima and tunica media, indicating successful induction of cardiovascular inflammation by choline chloride. These histological manifestations are consistent with published findings indicating that TMAO, derived from choline, L-carnitine, or phosphatidylcholine, induces vascular inflammation [3, 5, 8]. In contrast, following tangeretin treatment, aortic intimal thickening significantly decreased, smooth muscle cells were uniformly arranged, and no smooth muscle cell hyperplasia was observed. These results collectively demonstrate that tangeretin effectively prevents TMAO-induced cardiovascular inflammation. The results of our study also indicated that the CHO group showed significantly higher levels of TC (**Figure 1B**), TG (**Figure 1C**), LDL-C (**Figure 1D**) and lower level of HDL-C (**Figure 1E**) in serum lipid profiles than the NOR group. These changes reflected a gradual normalization of lipid metabolism and were positively correlated with histopathological alterations in the aorta. In this investigation, we assessed the protective efficacy of tangeretin on key antioxidant markers (SOD and CAT) (**Figure 1G, 1H**) and prooxidant marker (MDA) (**Figure 1F**), alongside its impact on pathological alterations in intestinal tissues. Notably, the CHO group showed a significant increase in MDA levels, coupled with a substantial decrease in enzymatic activity of SOD and CAT compared to the NOR group. This imbalance may contribute to the accumulation of reactive oxygen species (ROS), an escalation in MDA concentration, and increased susceptibility to intestinal mucosa damage [20]. Conversely, tangeretin administration showed a significant increase in the activity of SOD and CAT enzymes, concomitant with a decrease in MDA levels. Consequently, the observed intestinal protective effect of tangeretin is inferred to arise from its ability to mitigate lipoperoxidation, as evidenced by decreased levels of MDA, and restoration of SOD and CAT levels. This restorative action is attributed to the inhibitory effect of tangeretin on oxidative damage induced by choline chloride in the colonic mucosa of experimental rats.

Preprints (www.preprints.org) | NOT PEER-REVIEWED | Posted: 12 January 2024 doi:10.20944/preprints202401.0960.v1

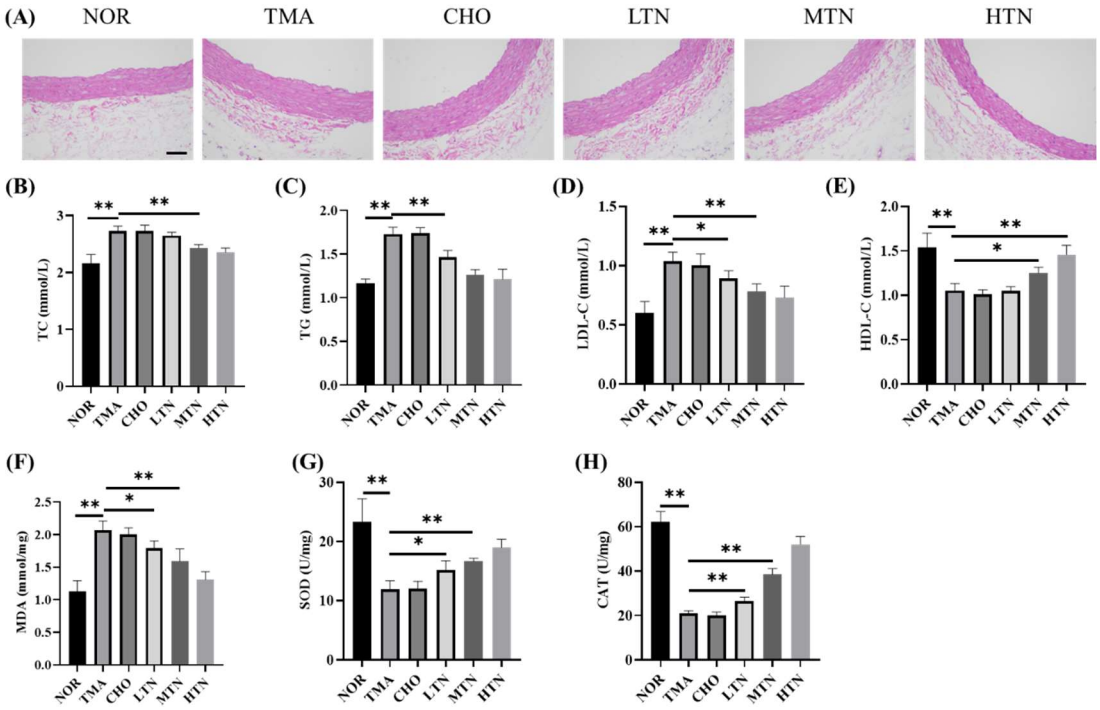

Figure 1. Aortic sinus HE staining results (200×, Scale bar = 200 μm) (A) and serum content of TC (B), TG (C), LDL-C (D), HDL-C (E), MDA (F), SOD (G), and CAT (H) (n=3-5. *p<0.05, **p<0.01).

The HE staining results (**Figure 2A**) illustrated that choline chloride administration induced aberrant goblet cell proliferation, lamina propria tissue damage, and villous atrophy in the intestine, ultimately leading to the disruption of submucosal architecture. Pathological findings in the CHO and TMA groups indicate a direct correlation between long-term dietary intake of choline and TMA production. However, tangeretin administration significantly ameliorated these abnormal goblet cell growth patterns. IHC staining results indicated that choline chloride reduced ZO-1 levels (**Figure 2**B, 2D) and Occludin levels (**Figure 2**C, 2E) in the ileum. Tangeretin treatment significantly increased the expression levels of ZO-1 (0.164 NOR, 0.049 CHO, 0.109 HTN) and Occludin (0.22 NOR, 0.107 CHO, 0.219 HTN), signifying an enhancement in intestinal tight junctions. Tight junction proteins play an essential role in stabilizing intercellular connections, preserving cell polarity, establishing specific apical domains, and controlling critical cellular activities such as proliferation, differentiation, and migration [21]. Alterations in tight junctions may be correlated with the magnitude of intestinal pathology [20]. In the present study, prolonged exposure to choline chloride resulted in increased levels of oxidative stress, culminating in a deficiency in intestinal tight junctions. This impairment significantly affected the integrity of the gut epithelial barrier.

Preprints (www.preprints.org) | NOT PEER-REVIEWED | Posted: 12 January 2024 doi:10.20944/preprints202401.0960.v1

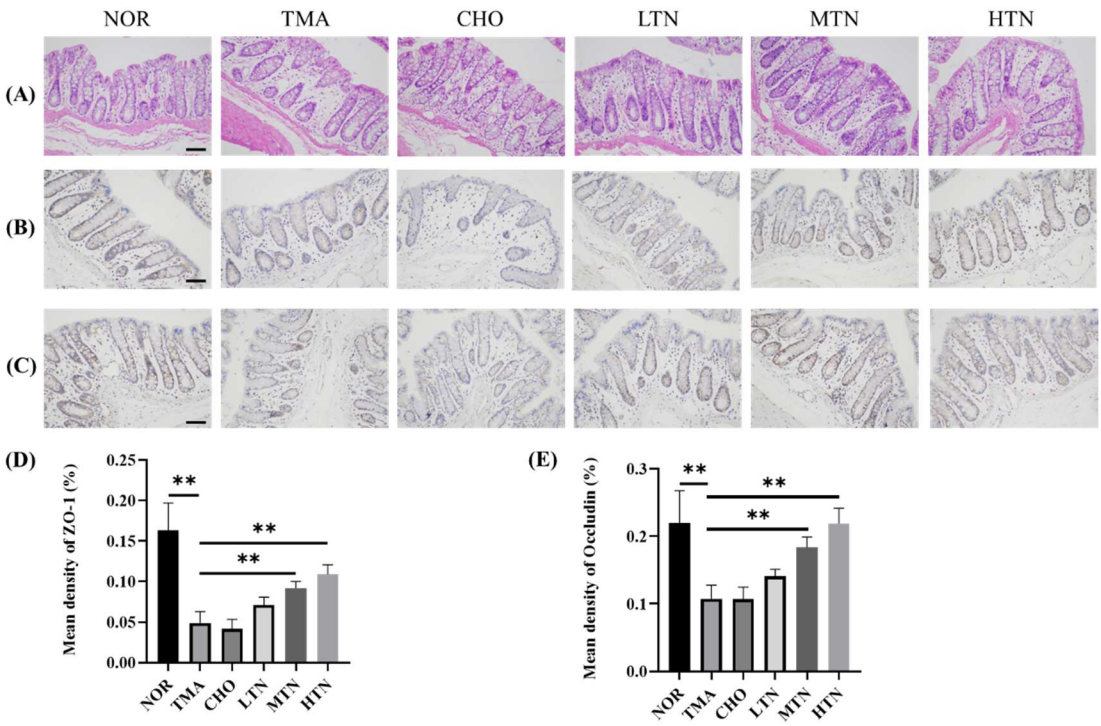

Figure 2. Ileal tissue HE and IHC results. (A) Examination of ileal tissue HE results. Immunohistochemistry (B) and quantification (D) of ZO-1. Immunohistochemistry (C) and quantification (E) of Occludin (200×). Scale bar = 200 μm, n=3-5. *p<0.05, **p<0.01.

3.2. Tangeretin Suppressed Choline Chloride-Stimulated Inflammation

Plasma levels of TNF-α, IL-1β, IL-6, IL-10, and IL-17, commonly used to assess inflammation severity, were significantly altered in CHO, which were reversed by the treatment of tangeretin, underscoring its potent anti-inflammatory effect (**Figure 3**A-E). RT-qPCR revealed that choline chloride treatment significantly upregulated TLR4, MyD88, and NF-κB expression by 7.48, 14.9, and 17.6 folds, respectively. In contrast, simultaneous administration of 200 mg/kg BW tangeretin led to a significant decrease in these transcript levels to 3.44, 2.44, and 3.36 folds, respectively (**Figure 3**F-H). These results suggest that tangeretin targets the TLR4\MyD88\NF-κB signaling pathway to inhibit the inflammatory response induced by long-term choline intake.

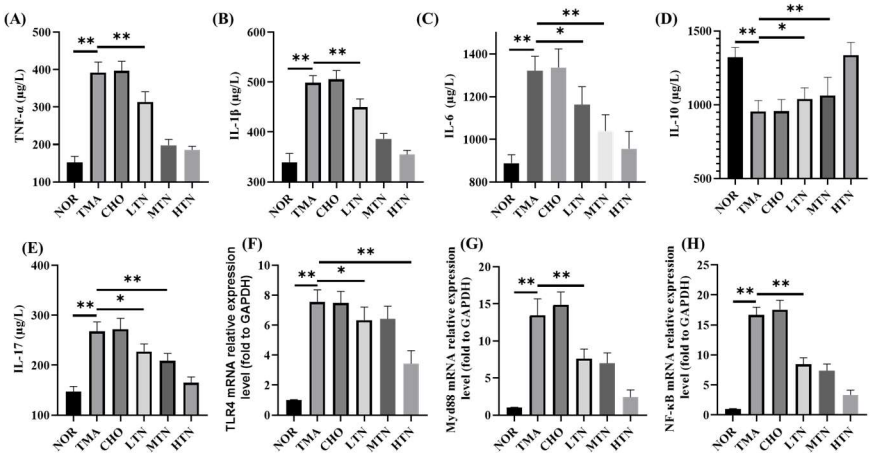

Figure 3. Plasma contents of TNF-α (A), IL-1β (B), IL-6 (C), IL-10 (D), IL-17 (E), and aortic TLR4 (F), MyD88 (G), NF-Kb (H) relative expression levels (n=3-5. *p<0.05, **p<0.01).

3.3. Tangeretin Regulated the Diversity of Intestinal Flora

Preprints (www.preprints.org) | NOT PEER-REVIEWED | Posted: 12 January 2024 doi:10.20944/preprints202401.0960.v1

PCA analysis (**Figure 4**A) indicated that the NOR group was distinct from the other groups, highlighting the impact of choline chloride treatment on intestinal flora composition. Clustering results of the tangeretin treatment groups differed from those of the CHO group or TMA group, revealing that tangeretin treatment altered the community structure of intestinal flora without completely reversing the changes caused by choline chloride treatment.

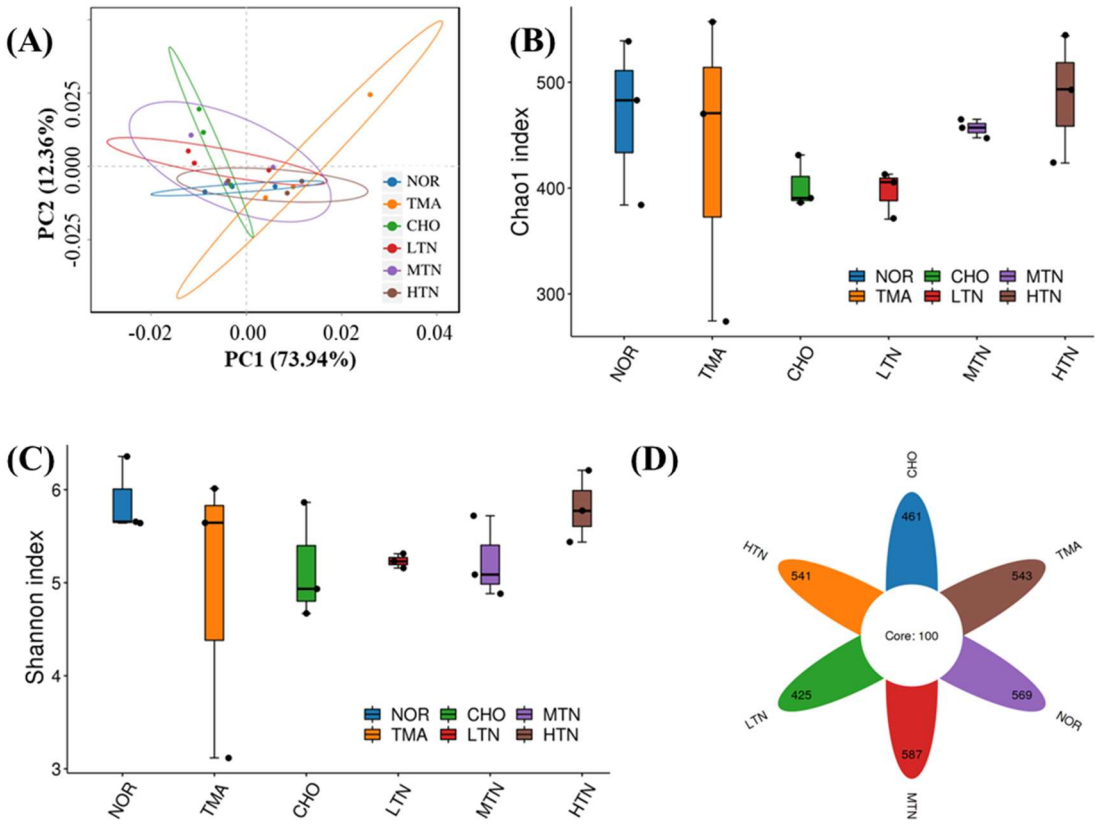

Figure 4. 16S rDNA sequence analysis of gut microbes. (A) β diversity analysis of Principal Coordinate Analysis, (B) α diversity analysis of Chao1 index, (C) Shannon diversity index, and (D) ASV Venn diagram.

Choline chloride reduced both the Chao1 index, reflecting species richness, and the Shannon diversity index, indicating evenness, in the intestinal flora of rats compared to NOR. After tangeretin treatment, the richness and evenness of the intestinal microflora exhibited a promising rise (**Figure 4**B and 4C). Fortunately, the results of **Figure 4**D revealed that the ASVs of the NOR, CHO, HTN, MTN, or LTN groups were 669, 561, 641, 687, and 525, respectively, indicating changes in gut microbiota composition with the intervention of tangeretin.

3.4. Tangeretin Modulated the Overall Structure and Composition of Gut Microbiota

At the genus level, the most significant changes in abundance were observed in *Christensenellaceae*, UCG 005, *Prevotellaceae*, *Bacillus*, unclassified Lachnospiraceae, *Clostridia*, *Prevotellaceae*, *Murihaculaceae*, *Lactobacillus*, and *Ligilactobacillus* (**Figure 5**A). Notably, bacteria involved in choline metabolism, such as *Clostridiaceae* and *Lactobacillus*, displayed significant downregulation upon treatment with tangeretin (**Figure 5**B, 5C). In our analysis of the differences in KEGG metabolic pathways between the CHO cohort and the HTN population, we observed that the differences and alterations in functional genes associated with cardiovascular disease were the most significant, with a *p*-value of < e-15 (**Figure 5**D). These findings indicated that tangeretin has the ability to affect the levels of gut commensals involved in choline metabolism into TMA, thereby mitigating valve damage from choline administration.

Preprints (www.preprints.org) | NOT PEER-REVIEWED | Posted: 12 January 2024 doi:10.20944/preprints202401.0960.v1

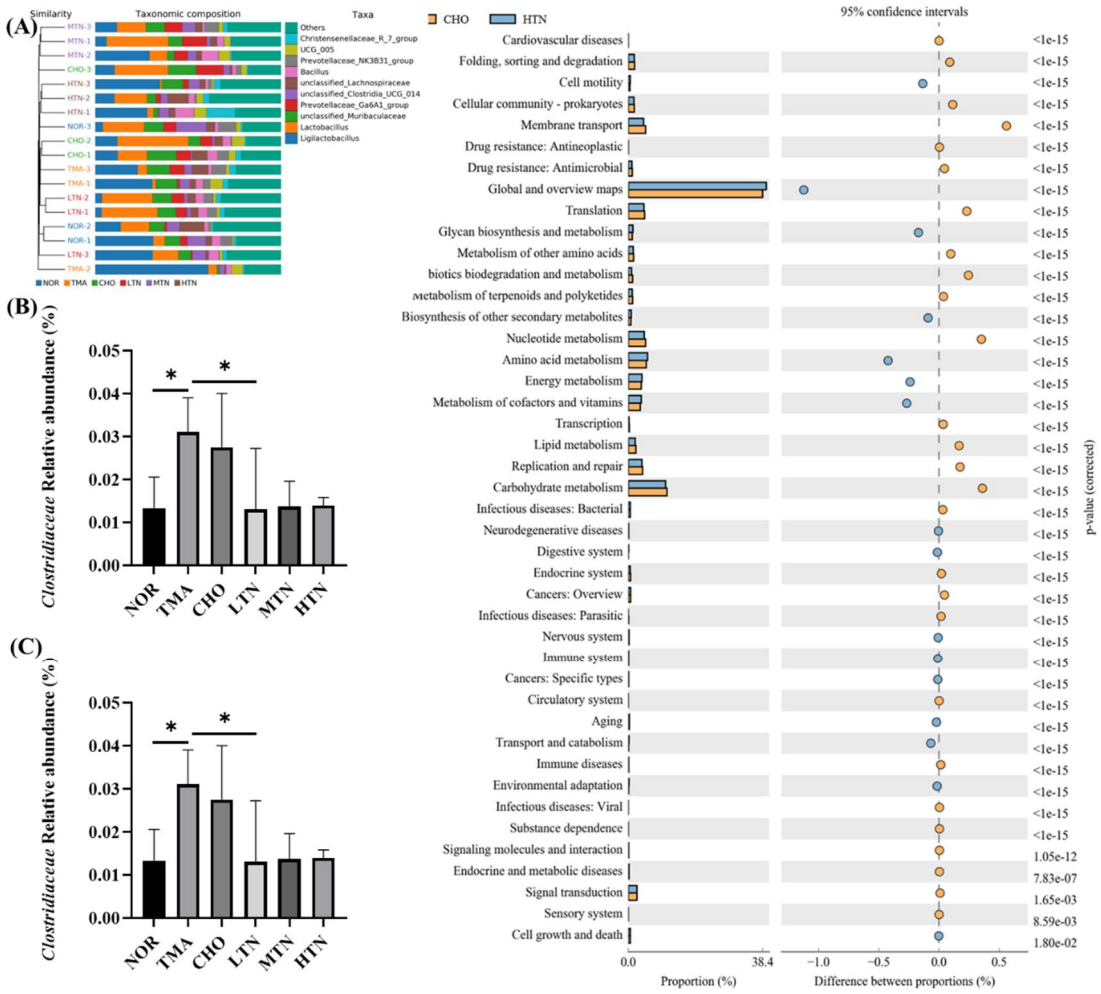

Figure 5. Tangeretin influenced the overall patterning and makeup of gut microbiota in rats treated with choline chloride. (A) Gut microbiota composition at the phylum level. (B) Relative abundance of Clostridiaceae. (C) Relative abundance of Lactobacillus. (D) Analysis of distinctions in metabolic pathways of KEGG. Data are illustrated as means ± SD, n=3-5. *p<0.05.

3.5. Tangeretin Inhibited the Conversion of Choline Chloride to TMA via CutC

In vitro experiments with *L. saccharolyticum* WM1 demonstrated its time-dependent conversion of choline to TMA (**Figure 6**A). Tangeretin significantly suppressed this conversion in a concentration-dependent inhibition manner (**Figure 6**B) and led to a reduction in serum TMAO levels (**Figure 6**C). In order to evaluate the simulated CutC protein, ERRAT scoring was used, where it obtained a value of 95.27. The PROCHECK analysis reported that 92.9% of amino acids exhibited acceptable conformations, indicating good structural integrity for the protein model. In addition, when juxtaposing the simulated structure with the I-TASSER structure, both protein models exhibited substantial similarity in the overall tertiary structure, albeit scattered structural transformations observed within N-terminal residues 1-60 (**Figure 6**D). Subsequently, for subsequent analyses, the Robetta-modelled structure was selected for docking studies. Interaction analysis revealed that tangeretin molecules interact primarily within the hydrophobic pocket of CutC protein. The docking simulations (**Figure 6**E) revealed a docking energy of -32.6549 kJ/mol for the tangeretin and CutC protein complex, exceeding the threshold of -29.301 kJ/mol [22]. This result indicates a strong binding relationship between tangeretin and CutC protein. Visualization of the docking results demonstrated that tangeretin established five conventional hydrogen bonds with amino acid residues TYR-87, ALA-136, and TYR-167 in CutC. The strong docking interaction between tangeretin and CutC implies the formation of substantial bonding forces and bonds, providing valuable insights into the structure-function relationship between tangeretin and CutC. Our findings confirm that

Preprints (www.preprints.org) | NOT PEER-REVIEWED | Posted: 12 January 2024 doi:10.20944/preprints202401.0960.v1

long-term high-dose choline chloride treatment disrupts the gut-blood barrier, facilitating increased gut-to-blood permeation of TMA, a toxic byproduct generated by gut flora. Significantly, our study suggests that elevated plasma levels of TMAO are a consequential consequence of elevated plasma TMA, a precursor to TMAO. This phenomenon arises from impaired intestinal barrier function in rats exposed to choline chloride.

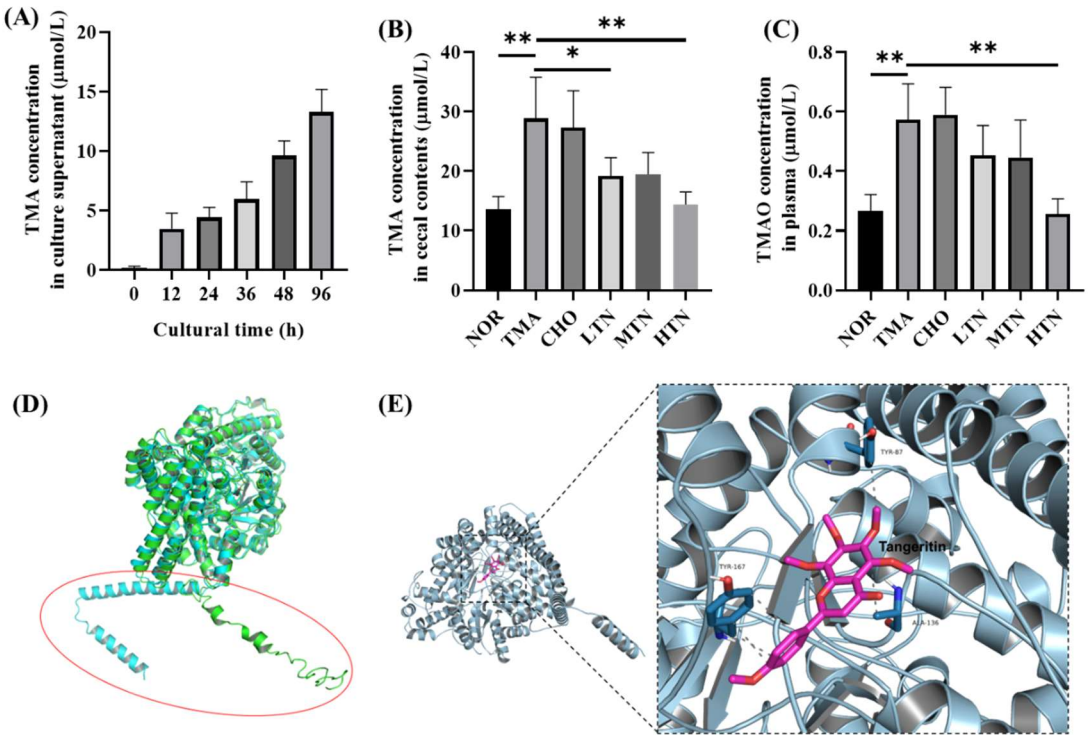

Figure 6. Detection of TMA and TMAO levels and molecular docking of tangeretin with CutC. (A) Plasma TMAO levels. (B) Cecal content TMA levels. (C) Cultural supernatant TMA level. (D) Computer generated structure of L. saccharolyticum WM1 CutC; (E) Interactions of tangeretin with important residues (n=3-5. *p<0.05, **p<0.01).

4. Conclusion

Both *in vivo* and *in vitro* demonstrations confirmed the defensive role of tangeretin against TMAO-induced cardiovascular inflammation. In our study, we convincingly validated that choline chloride induces vascular inflammation by upregulating TLR4/MyD88/NF-κB signaling, and treatment with tangeretin efficaciously inhibited these inflammatory biomarkers dose-dependently, thereby preventing tissue inflammation. Essentially, tangeretin treatment not only alleviated prolonged choline-induced damage to the intestinal mucosa, but also interfered with the intestinal microbiota-mediated conversion of choline into TMA. This dual mechanism contributes to its preventive activity against cardiovascular inflammation.

CRediT authorship contribution statement: Y. C. and W. L.: Conceptualization, methodology, writing - original draft; Y. C., C. L., K. L., and Y. L.: Investigation, project administration; K. L. and M. Z.: Formal analysis, validation; C. L. and M. Z.: Resources, software; X. S. and W. L.: Supervision, project administration, writing - review & editing.

Data Availability Statement: The database that supports the conclusions of this research work will be made available by the authors upon express request and with the authorization of the Ethics and Research Committee.

Acknowledgments: This research work was supported by the Grants from the Nature Science Foundation of Hubei Province (2022CFC057).

Conflicts of Interest: The authors declare no conflict of interest.

 doi:10.20944/preprints202401.0960.v1

References

1. Brennan, L., Castro, S., Brownson, R.C., Claus, J., Orleans, C.T., Accelerating evidence reviews and broadening evidence standards to identify effective, promising, and emerging policy and environmental strategies for prevention of childhood obesity, *Annu Rev Publ Health* **2011,** 32, 199-223.
2. Yang, G., Lin, C.C., Yang, Y., Yuan, L., Wang, P., Wen, X., Pan, M.H., Zhao, H., Ho, C.T., Li, S., Nobiletin prevents trimethylamine oxide-induced vascular inflammation via inhibition of the nf-κb/mapk pathways, *J Agr Food Chem* **2019,** 67, 6169-6176.
3. Wang, Z., Klipfell, E., Bennett, B.J., Koeth, R., Levison, B.S., Dugar, B., Feldstein, A.E., Britt, E.B., Fu, X., Chung, Y.M., Wu, Y., Schauer, P., Smith, J.D., Allayee, H., Tang, W.H., DiDonato, J.A., Lusis, A.J., Hazen, S.L., Gut flora metabolism of phosphatidylcholine promotes cardiovascular disease, *Nature* **2011,** 472, 57-63.
4. Koeth, R.A., Wang, Z., Levison, B.S., Buffa, J.A., Org, E., Sheehy, B.T., Britt, E.B., Fu, X., Wu, Y., Li, L., Smith, J.D., DiDonato, J.A., Chen, J., Li, H., Wu, G.D., Lewis, J.D., Warrier, M., Brown, J.M., Krauss, R.M., Tang, W.H., Bushman, F.D., Lusis, A.J., Hazen, S.L., Intestinal microbiota metabolism of l-carnitine, a nutrient in red meat, promotes atherosclerosis, *Nat Med* **2013,** 19, 576-585.
5. Tang, W.H., Wang, Z., Levison, B.S., Koeth, R.A., Britt, E.B., Fu, X., Wu, Y., Hazen, S.L., Intestinal microbial metabolism of phosphatidylcholine and cardiovascular risk, *N Engl J Med* **2013,** 368, 1575-1584.
6. Vaiyapuri, S., Roweth, H., Ali, M.S., Unsworth, A.J., Stainer, A.R., Flora, G.D., Crescente, M., Jones, C.I., Moraes, L.A., Gibbins, J.M., Pharmacological actions of nobiletin in the modulation of platelet function, *Brit J Pharmacol* **2015,** 172, 4133-4145.
7. Roberts, A.B., Gu, X., Buffa, J.A., Hurd, A.G., Wang, Z., Zhu, W., Gupta, N., Skye, S.M., Cody, D.B., Levison, B.S., Barrington, W.T., Russell, M.W., Reed, J.M., Duzan, A., Lang, J.M., Fu, X., Li, L., Myers, A.J., Rachakonda, S., DiDonato, J.A., Brown, J.M., Gogonea, V., Lusis, A.J., Garcia-Garcia, J.C., Hazen, S.L., Development of a gut microbe-targeted nonlethal therapeutic to inhibit thrombosis potential, *Nat Med* **2018,** 24, 1407-1417.
8. Cai, Y.Y., Huang, F.Q., Lao, X., Lu, Y., Gao, X., Alolga, R.N., Yin, K., Zhou, X., Wang, Y., Liu, B., Shang, J., Qi, L.W., Li, J., Integrated metagenomics identifies a crucial role for trimethylamine-producing lachnoclostridium in promoting atherosclerosis, *NPJ Biofilms Microbi* **2022,** 8, 11.
9. Jonsson, A.L., Bäckhed, F., Role of gut microbiota in atherosclerosis, *Nat Rev Cardiol* **2017,** 14, 79-87.
10. Yang, G., Xia, X., Zhong, H., Shen, J., Li, S., Protective effect of tangeretin and 5-hydroxy-6,7,8,3',4'-pentamethoxyflavone on collagen-induced arthritis by inhibiting autophagy via activation of the ros-akt/mtor signaling pathway, *J Agr Food Chem* **2021,** 69, 259-266.
11. Zhang, M., Zhang, X., Zhu, J., Zhao, D.G., Ma, Y.Y., Li, D., Ho, C.T., Huang, Q., Bidirectional interaction of nobiletin and gut microbiota in mice fed with a high-fat diet, *Food Funct* **2021,** 12, 3516-3526.
12. Alsaif, M.A., Khan, L.A., Alhamdan, A.A., Alorf, S., Al-Othman, A.M., Alawami, S., Effects of dietary flavonoids intake in saudi patients with coronary heart disease, *J Family Community Med* **2007,** 14, 119-126.
13. Caporaso, J.G., Kuczynski, J., Stombaugh, J., Bittinger, K., Bushman, F.D., Costello, E.K., Fierer, N., Peña, A.G., Goodrich, J.K., Gordon, J.I., Huttley, G.A., Kelley, S.T., Knights, D., Koenig, J.E., Ley, R.E., Lozupone, C.A., McDonald, D., Muegge, B.D., Pirrung, M., Reeder, J., Sevinsky, J.R., Turnbaugh, P.J., Walters, W.A., Widmann, J., Yatsunenko, T., Zaneveld, J., Knight, R., Qiime allows analysis of high-throughput community sequencing data, *Nat methods* **2010,** 7, 335-336.
14. Edgar, R.C., Search and clustering orders of magnitude faster than blast, *Bioinformatics* **2010,** 26, 2460-2461.
15. Lozupone, C.A., Hamady, M., Kelley, S.T., Knight, R., Quantitative and qualitative beta diversity measures lead to different insights into factors that structure microbial communities, *Appl Environ Microb* **2007,** 73, 1576-1585.
16. Huson, D.H., Mitra, S., Ruscheweyh, H.J., Weber, N., Schuster, S.C., Integrative analysis of environmental sequences using megan4, *Genome Res* **2011,** 21, 1552-1560.
17. Asnicar, F., Weingart, G., Tickle, T.L., Huttenhower, C., Segata, N., Compact graphical representation of phylogenetic data and metadata with graphlan, *PeerJ* **2015,** 3, e1029.
18. Hamidi, B., Wallace, K., Vasu, C., Alekseyenko, A.V., W(∗)(d) -test: Robust distance-based multivariate analysis of variance, *Microbiome* **2019,** 7, 51.
19. Ocque, A.J., Stubbs, J.R., Nolin, T.D., Development and validation of a simple uhplc-ms/ms method for the simultaneous determination of trimethylamine n-oxide, choline, and betaine in human plasma and urine, *J Pharm Biomed Anal* **2015,** 109, 128-135.
20. Guzmán-Gómez, O., García-Rodríguez, R.V., Pérez-Gutierrez, S., Rivero-Ramírez, N.L., García-Martínez, Y., Pablo-Pérez, S.S., Pérez-Pastén-Borja, R., Cristóbal-Luna, J.M., Chamorro-Cevallos, G., Protective effect of the phycobiliproteins from arthrospira maxima on indomethacin-induced gastric ulcer in a rat model, *Plants* **2023,** 12, 1586.
21. Kirschner, N., Poetzl, C., von den Driesch, P., Wladykowski, E., Moll, I., Behne, M.J., Brandner, J.M., Alteration of tight junction proteins is an early event in psoriasis: Putative involvement of proinflammatory cytokines, *Am J Pathol* **2009,** 175, 1095-1106.

 doi:10.20944/preprints202401.0960.v1

22. He, S., He, X., Pan, S., Jiang, W., Exploring the mechanism of chuanxiong rhizoma against thrombosis based on network pharmacology, molecular docking and experimental verification, *Molecules* **2023,** 28, 6702.